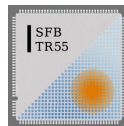


QCD transition in magnetic fields

Gergely Endrődi

University of Regensburg



Advances in Strong-Field Electrodynamics
Budapest, 3rd-6th February 2014

Outline - first part

- introduction
 - ▶ strong interactions at finite temperature
 - ▶ quark-gluon plasma exposed to magnetic fields
 - ▶ appetizer: chiral magnetic effect in heavy-ion collisions
 - ▶ approaches to study QCD
- free case: energy levels
 - ▶ non-relativistic case, infinite volume
 - ▶ relativistic case, infinite volume
 - ▶ relativistic case, on the torus
 - ▶ Hofstadter's butterfly
- free case, thermodynamic potential
 - ▶ representation at finite T with Matsubara frequencies
 - ▶ treatment via Mellin transformation
 - ▶ alternative derivation: Schwinger proper-time method
 - ▶ alternative representation: with energies
 - ▶ charge renormalization vs B -dependent divergences
 - ▶ observables derived from $\log \mathcal{Z}$

Outline - second part

- numerical results I: phase diagram
 - ▶ symmetries and order parameters
 - ▶ predictions from effective theories and models
 - ▶ magnetic catalysis and inverse catalysis
 - ▶ transition temperature, nature of transition at nonzero B
- numerical results II: equation of state
 - ▶ concept of the pressure in magnetic fields
 - ▶ magnetization, magnetic susceptibility
 - ▶ comparison to hadron resonance gas model
 - ▶ squeezing-effect in heavy-ion collisions
- numerical results III: chiral magnetic effect
 - ▶ electric polarization of CP-odd domains
 - ▶ comparison to model predictions

Literature

- Landau-Lifshitz Vol.3 Quantum mechanics, chapter XV.
(non-relativistic eigenvalue problem)
- Akhiezer, Berestetskii: Quantum electrodynamics, chapter 12.
(relativistic eigenvalue problem)
- Kapusta: Finite-temperature field theory, chapter 2.
(functional integral for fermions/bosons)
- Al-Hashimi, Wiese: “Discrete accidental symmetry for a particle in a constant magnetic field on a torus”
- Hofstadter: “Energy levels and wavefunctions of Bloch electrons in rational and irrational magnetic fields”
- Schwinger: “On gauge invariance and vacuum polarization”
- Dunne: “Heisenberg-Euler effective Lagrangians: basics and extensions”

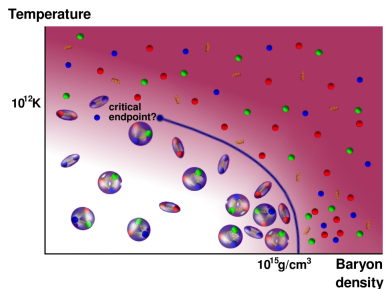
QCD and quark-gluon plasma

- elementary particle interactions:
gravitational, electromagnetic, weak, strong
Standard Model
- strong sector: Quantum Chromodynamics
- elementary particles: quarks (\sim electrons) and gluons (\sim photons)
but: they cannot be observed directly
 \Rightarrow *confinement* at low temperatures
- asymptotic freedom [Gross, Politzer, Wilczek '04]
 \Rightarrow heating or compressing the system leads to *deconfinement*: quark-gluon plasma is formed
- transition between the two phases
characteristics: order (1st/2nd/crossover)
critical temperature T_c
equation of state



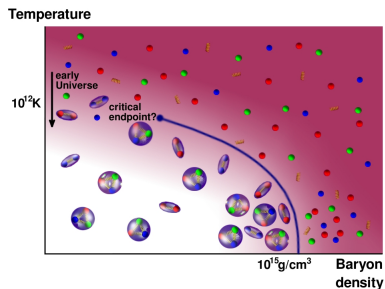
QCD phase diagram

- why is the physics of the quark-gluon plasma interesting?
 - ▶ large T : early Universe, cosmological models
 - ▶ large ρ : neutron stars
 - ▶ large T and/or ρ : heavy-ion collisions, experiment design



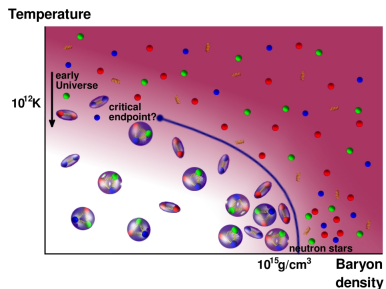
QCD phase diagram

- why is the physics of the quark-gluon plasma interesting?
 - ▶ large T : early Universe, cosmological models
 - ▶ large ρ : neutron stars
 - ▶ large T and/or ρ : heavy-ion collisions, experiment design



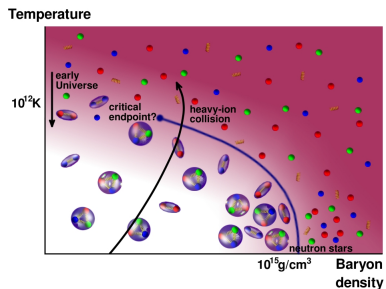
QCD phase diagram

- why is the physics of the quark-gluon plasma interesting?
 - ▶ large T : early Universe, cosmological models
 - ▶ large ρ : neutron stars
 - ▶ large T and/or ρ : heavy-ion collisions, experiment design



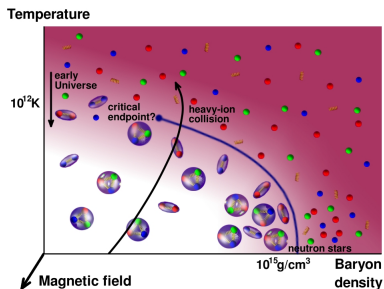
QCD phase diagram

- why is the physics of the quark-gluon plasma interesting?
 - ▶ large T : early Universe, cosmological models
 - ▶ large ρ : neutron stars
 - ▶ large T and/or ρ : heavy-ion collisions, experiment design



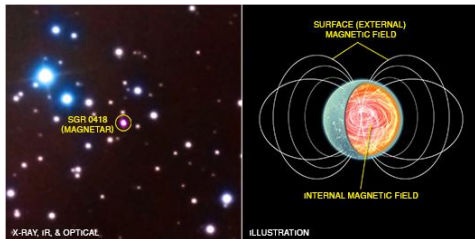
QCD phase diagram

- why is the physics of the quark-gluon plasma interesting?
 - ▶ large T : early Universe, cosmological models
 - ▶ large ρ : neutron stars
 - ▶ large T and/or ρ : heavy-ion collisions, experiment design



- additional, relevant parameter:
 - ▶ external magnetic field B

Example 1: neutron star



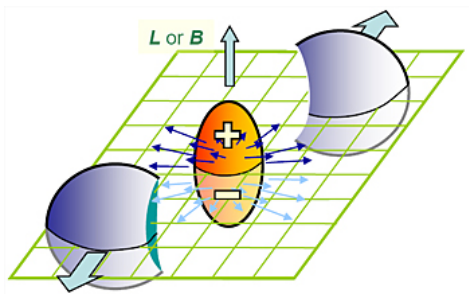
[Rea et al. '13]

- possible quark core at center with high density, low temperature
- magnetars: extreme strong magnetic fields

Typical magnetic fields

- magnetic field of Earth 10^{-5} T
- common magnet 10^{-3} T
- strongest human-made field in lab 10^2 T
- magnetar surface 10^{10} T
- magnetar core ?

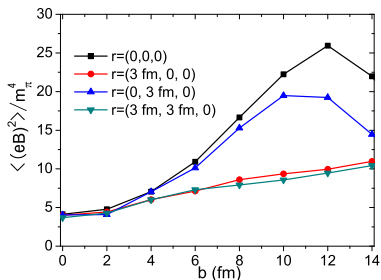
Example 2: heavy-ion collision



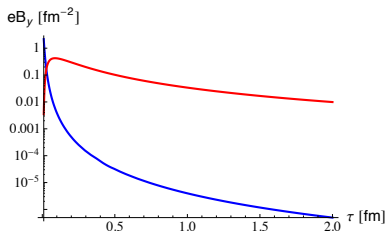
[STAR collaboration, '10]

- off-central collisions generate magnetic fields: strength controlled by \sqrt{s} and impact parameter (centrality)
- strong (but very uncertain) time-dependence
- anisotropic spatial gradients

Example 2: heavy-ion collision



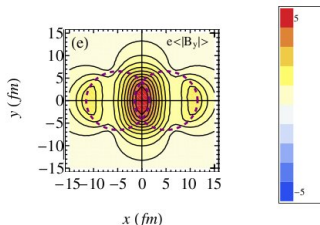
[Bloczynski et al. '12]



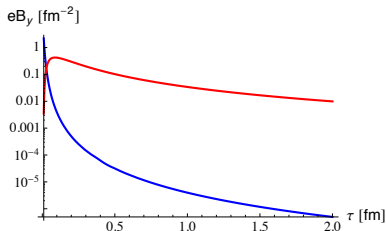
[Gursoy et al '13]

- off-central collisions generate magnetic fields: strength controlled by \sqrt{s} and impact parameter (centrality)
- strong (but very uncertain) time-dependence
- anisotropic spatial gradients

Example 2: heavy-ion collision



[Deng et al '12]



[Gursoy et al '13]

- off-central collisions generate magnetic fields: strength controlled by \sqrt{s} and impact parameter (centrality)
- strong (but very uncertain) time-dependence
- anisotropic spatial gradients

Typical magnetic fields

- magnetic field of Earth 10^{-5} T
- common magnet 10^{-3} T
- strongest man-made field in lab 10^2 T
- magnetar surface 10^{10} T
- magnetar core ?
- LHC Pb-Pb at 2.7 TeV, $b = 10$ fm [Skokov '09] 10^{15} T

convert: 10^{15} T $\approx 10m_{\pi}^2 \approx 2\Lambda_{\text{QCD}}^2$

\Rightarrow electromagnetic and strong interactions can compete

Chiral magnetic effect

- QCD is parity-symmetric (neutron EDM $< 10^{-26} e \text{ cm}$)

$$\mathcal{L}_{\text{QCD}} = \sum_f \bar{\psi}_f (\not{D} + m_f) \psi_f + \frac{1}{2} \text{Tr} F_{\mu\nu} F_{\mu\nu} + \theta \cdot \underbrace{\frac{1}{16\pi^2} \text{Tr} F_{\mu\nu} \tilde{F}_{\mu\nu}}_{Q_{\text{top}}}$$

$\Rightarrow \theta < 10^{-10}$ (strong CP problem)

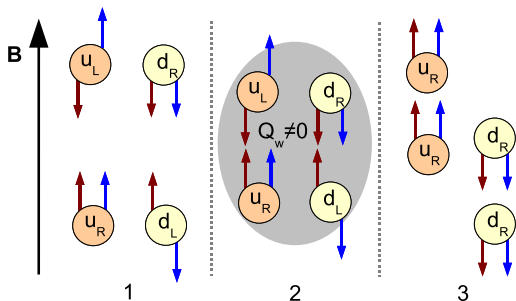
- axial anomaly

$$N_R - N_L \equiv \int d^4x \partial_\mu j^{\mu 5} = 2Q_{\text{top}}$$

\Rightarrow topology converts between left- and right-handed quarks

Chiral magnetic effect

- local CP-violation through domains with $Q_{\text{top}} \neq 0$?
- detect them through magnetic field B [Kharzeev et al. '08]

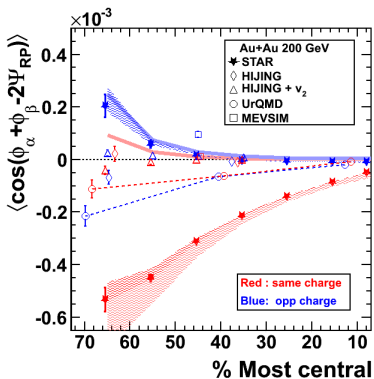
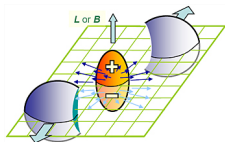


1. quarks interact with B : spins aligned
2. quarks interact with topology: chiralities (helicities) “aligned”
3. result: charge separation

Chiral magnetic effect

- Q_{top} -domains fluctuate, direction of B fluctuates
 \Rightarrow effect vanishes on average
- correlations may survive ($\alpha, \beta = \pm$)

$$a_{\alpha\beta} = -\cos[(\Phi_\alpha - \Psi_{\text{RP}}) + (\Phi_\beta - \Psi_{\text{RP}})]$$



[STAR collaboration '09]

- need 3-particle correlations (technically complicated)
- CME prediction:

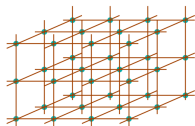
$$a_{++} = a_{--} = -a_{+-} > 0$$
- CP-even backgrounds should be subtracted

Approaches to study QCD

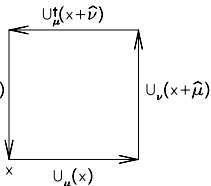
- various methods in various regimes:
 - ▶ high T/B : perturbation theory
 - ▶ low T/B : chiral perturbation theory, hadronic models
 - ▶ transition region: non-perturbative methods, lattice gauge theory [Wilson, '74]

- discretize quark and gluon fields ψ and A_μ on a 4D space-time lattice with spacing a

- ▶ use $U_\mu = e^{iaA_\mu}$ instead of A_μ
- ▶ U_μ : links, ψ : sites



- example: gauge action $F_{\mu\nu}F_{\mu\nu}(x) \sim U_\mu^\dagger(x)$



Lattice simulations

- functional integral

$$\mathcal{Z} = \int \mathcal{D}U_\mu \mathcal{D}\bar{\psi} \mathcal{D}\psi \exp\left(-\int d^4x \mathcal{L}_{\text{QCD}}\right)$$

Lattice simulations

- functional integral

$$\mathcal{Z} = \int \mathcal{D}U_\mu \exp \left(- \int d^4x \frac{1}{2} \text{Tr} F_{\mu\nu} F_{\mu\nu} \right) \cdot \prod_f \det \left(\not{D} + m_f^{\text{lat}} \right)$$

Lattice simulations

- functional integral

$$\mathcal{Z} = \int \mathcal{D}U_\mu \exp \left(- \int d^4x \frac{1}{2} \text{Tr} F_{\mu\nu} F_{\mu\nu} \right) \cdot \prod_f \det \left(\not{D} + m_f^{\text{lat}} \right)$$

- \mathcal{Z} analogous to partition function of a 4D statistical physics system; temperature and volume given as

$$T = 1/(N_t a), \quad V = (N_s a)^3$$

- continuum limit with T and V fix:

$$a \rightarrow 0 \quad \leftrightarrow \quad N_s, N_t \rightarrow \infty, N_s/N_t = \text{fix}$$

- \mathcal{Z} becomes a $\sim 10^9$ dimensional integral
 - ▶ importance sampling with weight e^{-S}
 - ▶ Monte-Carlo methods

Lattice simulations

- besides continuum limit, the biggest challenge is to simulate at the physical point: set m_f^{lat} such that the measured $m_\pi, m_\rho, m_\rho, \dots$ are the same as in nature
- typical computational requirement $\mathcal{O}(10 \text{ Tflop/s} \times \text{year})$



$\mathcal{O}(40 \text{ mio. core hours})$



$\mathcal{O}(100 \text{ GPU} \times \text{year})$

Outline - first part

- introduction
 - ▶ strong interactions at finite temperature
 - ▶ quark-gluon plasma exposed to magnetic fields
 - ▶ appetizer: chiral magnetic effect in heavy-ion collisions
 - ▶ approaches to study QCD
- free case: energy levels
 - ▶ non-relativistic case, infinite volume
 - ▶ relativistic case, infinite volume
 - ▶ relativistic case, on the torus
 - ▶ Hofstadter's butterfly
- free case, thermodynamic potential
 - ▶ representation at finite T with Matsubara frequencies
 - ▶ treatment via Mellin transformation
 - ▶ alternative derivation: Schwinger proper-time method
 - ▶ alternative representation: with energies
 - ▶ charge renormalization vs B -dependent divergences
 - ▶ observables derived from $\log \mathcal{Z}$

Energy eigenvalues

- non-relativistic case, infinite volume

$$E_n = \frac{p_z^2}{2m} + 2|qB|(n + 1/2 - \sigma_z), \quad \#_n = \infty$$

- relativistic case, infinite volume

$$E_n = \sqrt{p_z^2 + m^2 + 2|qB|(n + 1/2 - \sigma_z)}, \quad \#_n = \infty$$

- relativistic case, finite volume (torus)

$$E_n = \sqrt{p_z^2 + m^2 + 2|qB|(n + 1/2 - \sigma_z)}, \quad \#_n = \frac{|qB| \cdot L^2}{2\pi}$$

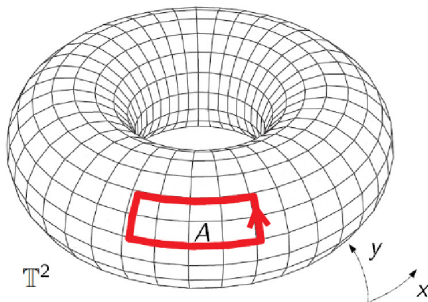
Magnetic flux quantization

- finite volume, continuum:

$$L^2 \cdot qB = \Phi = 2\pi N_b, \quad N_b \in \mathbb{Z}$$

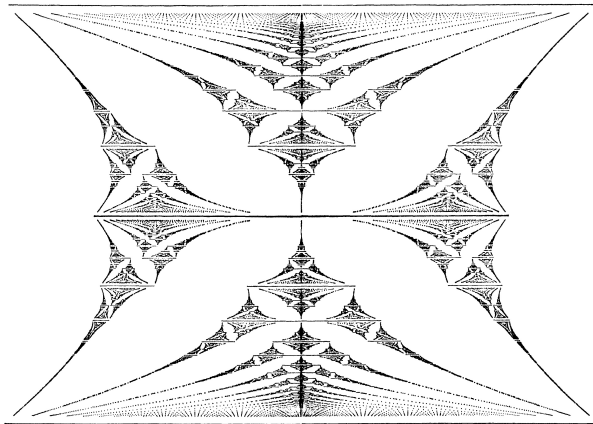
- finite volume, lattice:

$$(N_s a)^2 \cdot qB = \Phi = 2\pi N_b, \quad 0 < N_b < N_s^2$$

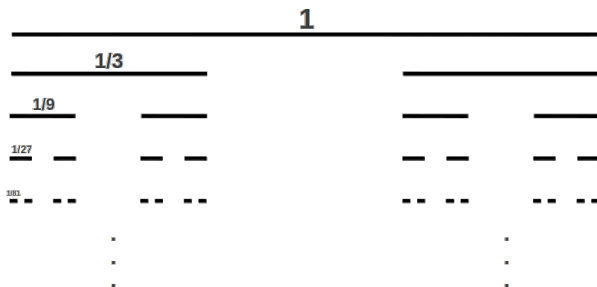


picture from [D'Elia et al '11]

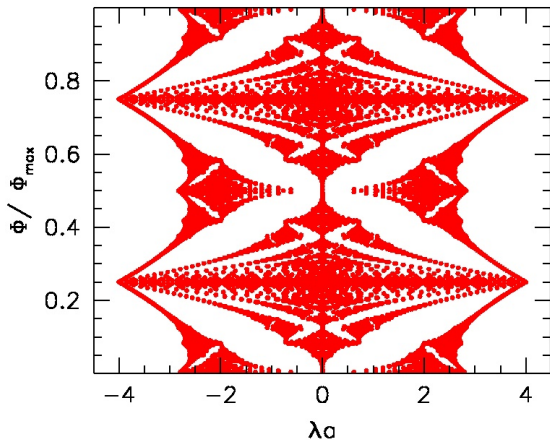
Hofstadter's butterfly



Hofstadter's butterfly and the Cantor set

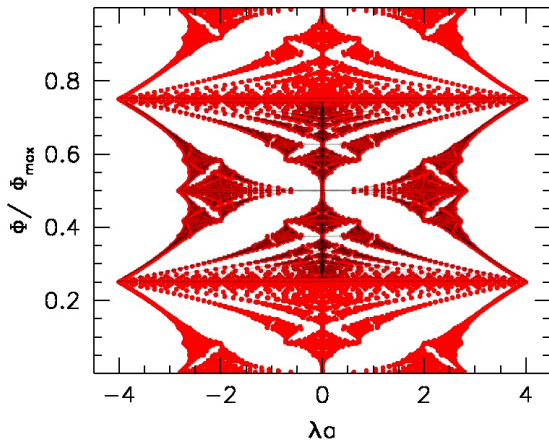


Hofstadter's cocoon on the lattice



- lattice flux quantized: $(N_s a)^2 q B = \Phi = 2\pi N_b$
 - ▶ infinite volume limit releases the butterfly
 - ▶ continuum limit kills the butterfly

Hofstadter's cocoon on the lattice



- lattice flux quantized: $(N_s a)^2 q B = \Phi = 2\pi N_b$
 - ▶ infinite volume limit releases the butterfly
 - ▶ continuum limit kills the butterfly

Free energies

- charged spin $-1/2$ particle

$$f^{(1/2)}(T, B) = + \frac{1}{8\pi^2} \int \frac{ds}{s^3} e^{-m^2 s} \cdot \frac{qBs \cdot \cosh(qBs)}{\sinh(qBs)} \cdot \Theta_3 \left[\frac{\pi}{2}, e^{-1/(4sT^2)} \right]$$

- charged spin -0 particle

$$f^{(0)}(T, B) = - \frac{1}{8\pi^2} \int \frac{ds}{s^3} e^{-m^2 s} \cdot \frac{qBs \cdot 1}{\sinh(qBs)} \cdot \Theta_3 \left[0, e^{-1/(4sT^2)} \right]$$

- in general, for spin $-\sigma$:

$$f^{(\sigma)}(T, B) = (-1)^\sigma \frac{qB}{2\pi} \sum_n \sum_{\sigma_z = -\sigma}^{\sigma} \int \frac{dp_z}{2\pi} \left[E_n + 2T \log \left(1 + e^{-E_n/T} \right) \right]$$

$$E_n = \sqrt{p_z^2 + m^2 + 2qB(n + 1/2 - \sigma_z)}$$

Renormalization at zero temperature

- calculate change in f : subtract $B = 0$ contribution
- charge renormalization at $\mathcal{O}(B^2)$

$$\begin{aligned}\Delta f^{(1/2)}(0, B) &= \frac{B^2}{2} + \frac{qB}{8\pi^2} \int \frac{ds}{s^2} e^{-m^2 s} \cdot \left[\coth(qBs) - \frac{1}{qBs} \right] \\ &= \frac{B_r^2}{2} + \frac{qB}{8\pi^2} \int \frac{ds}{s^2} e^{-m^2 s} \cdot \left[\coth(qBs) - \frac{1}{qBs} - \frac{qBs}{3} \right]\end{aligned}$$

- wave-function renormalization

$$B^2 = Z_q^{(1/2)} B_r^2, \quad Z_q^{(1/2)} = 1 + q_r^2 \cdot \beta_1^{(1/2)} \cdot \log \left(\frac{m^2}{\Lambda^2} \right)$$

- Ward identity

$$qB = q_r B_r, \quad q^2 = \frac{1}{Z_q^{(1/2)}} q_r^2$$

Renormalization

- expansion in the external field B diagrammatically
- $\mathcal{O}(B^0)$ contains B -independent divergences
- $\mathcal{O}(B^4)$ term is finite

▶ in the free case (1-loop)

The diagram shows the expansion of a double-line loop (two concentric circles) into a series of terms: a single-line loop, a loop with two external wavy lines, and a loop with four external wavy lines, followed by an ellipsis.

▶ $\mathcal{O}(B^2)$ term $\propto q^2 \cdot \beta_1$

Renormalization

- expansion in the external field B diagrammatically
- $\mathcal{O}(B^0)$ contains B -independent divergences
- $\mathcal{O}(B^4)$ term is finite

▶ with an internal photon to 2-loop

$$\text{Diagram with double line} = \text{Diagram with wavy line} + \text{Diagram with wavy line and two external wavy lines} + \text{Diagram with wavy line and four external wavy lines} + \dots$$

▶ $\mathcal{O}(B^2)$ term $\propto q^4 \cdot \beta_2$

Renormalization

- expansion in the external field B diagrammatically
- $\mathcal{O}(B^0)$ contains B -independent divergences
- $\mathcal{O}(B^4)$ term is finite

▶ with an internal gluon to 2-loop

$$\text{Diagram 1} = \text{Diagram 2} + \text{Diagram 3} + \text{Diagram 4} + \dots$$

▶ $\mathcal{O}(B^2)$ term $\propto q^2 \cdot g^2 \cdot \beta_{1,1}$

Renormalization

- expansion in the external field B diagrammatically
- $\mathcal{O}(B^0)$ contains B -independent divergences
- $\mathcal{O}(B^4)$ term is finite

▶ with an internal gluon to 2-loop

$$\text{Diagram 1} = \text{Diagram 2} + \text{Diagram 3} + \text{Diagram 4} + \dots$$

▶ $\mathcal{O}(B^2)$ term $\propto q^2 \cdot g^2 \cdot \beta_{1,1}$

- the coefficient of $\mathcal{O}(B^2)$ term equals the QED β -function (with QCD corrections)
 \Rightarrow background field method [Abbott '81]

Renormalization – summary

- even though B is very similar to a chemical potential, it undergoes wavefunction renormalization
- B -dependent divergence $\propto (qB)^2 \beta \log(\Lambda)$, which redefines the pure magnetic energy $B_r^2/2$
- implication: susceptibility χ_B vanishes at zero T
- in the free case, UV ($\Lambda \rightarrow \infty$) and IR ($m \rightarrow 0$) divergences are intertwined
 \Rightarrow quarks in SB limit are paramagnetic

$$\chi_B \propto \beta_1 \log(T/m) > 0$$

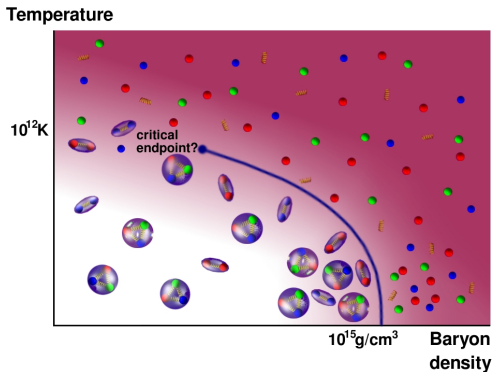
\Rightarrow magnetic catalysis of the quark condensate at $T = 0$

$$\mathcal{O}((qB)^2) : \quad \Delta \bar{\psi} \psi \propto \beta_1 > 0$$

Outline - second part

- numerical results I: phase diagram
 - ▶ symmetries and order parameters
 - ▶ predictions from effective theories and models
 - ▶ magnetic catalysis and inverse catalysis
 - ▶ transition temperature, nature of transition at nonzero B
- numerical results II: equation of state
 - ▶ concept of the pressure in magnetic fields
 - ▶ magnetization, magnetic susceptibility
 - ▶ comparison to hadron resonance gas model
 - ▶ squeezing-effect in heavy-ion collisions
- numerical results III: chiral magnetic effect
 - ▶ electric polarization of CP-odd domains
 - ▶ comparison to model predictions

QCD phase diagram



- how to map out the transition line?

Observables sensitive to transition

- chiral condensate
→ chiral symmetry breaking $m = 0$

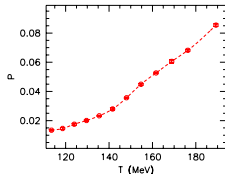
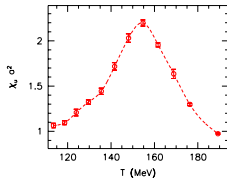
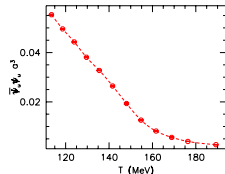
$$\bar{\psi}_f \psi_f = \frac{\partial \log \mathcal{Z}}{\partial m_f}$$

- chiral susceptibility
→ chiral symmetry breaking $m = 0$

$$\chi_f = \frac{\partial^2 \log \mathcal{Z}}{\partial m_f^2}$$

- Polyakov loop
→ deconfinement “ $m = \infty$ ”

$$P = \text{Tr} \exp \left[\int A_4(x, t) dt \right]$$



Magnetic catalysis

- what happens to $\bar{\psi}\psi$ ($\langle +q \uparrow, -q \downarrow \rangle$) in magnetic field?
 \Rightarrow magnetic moments parallel, energetically favored state (cf. Cooper-pairs in superconductors: Meissner effect)
- dimensional reduction $3 + 1 \rightarrow 1 + 1$ in the LLL

$$E_{LLL} = \sqrt{p_z^2 + m^2}, \quad s_{z,LLL} = +1/2, \quad \#_{LLL} = \frac{|qB| \cdot L_x L_y}{2\pi}$$

- chiral condensate \leftrightarrow spectral density around 0 [Banks, Casher '80]

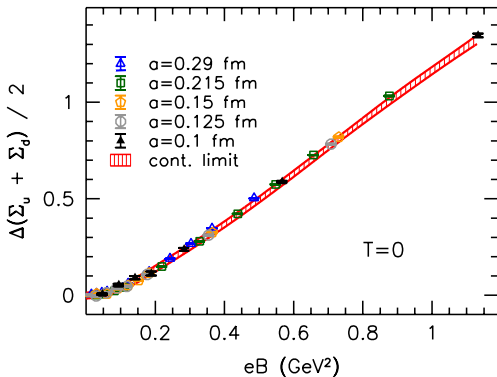
$$\bar{\psi}\psi \propto \rho(0)$$

- in the chiral limit, to maintain $\bar{\psi}\psi > 0$ (NJL [Gusynin et al '96])

$$\begin{array}{lll} B = 0 & \rho(p) \sim p^2 dp & \text{"we need a strong interaction"} \\ B \gg m^2 & \rho(p) \sim qB dp & \text{"the weakest interaction suffices"} \end{array}$$

Magnetic catalysis – zero temperature

- MC at zero temperature is a robust concept:
 χ PT, NJL, AdS-CFT, linear σ , lattice QCD at physical/unphysical m_π , ...

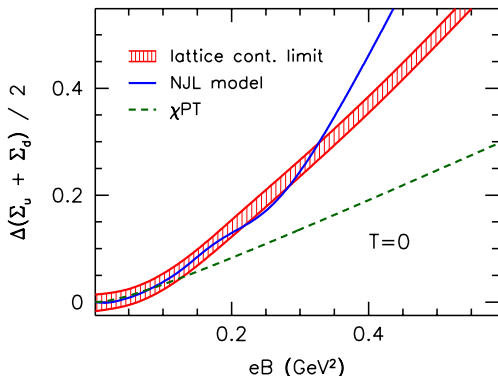


lattice QCD, physical m_π , continuum limit

[Bali,Bruckmann,Endrödi,Fodor,Katz,Schäfer '12]

Magnetic catalysis – zero temperature

- MC at zero temperature is a robust concept:
 χ PT, NJL, AdS-CFT, linear σ , lattice QCD at physical/unphysical m_π , ...

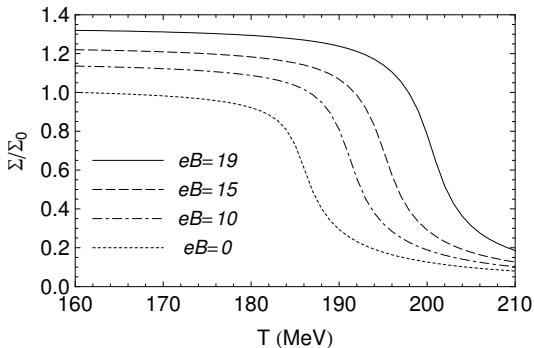


lattice QCD, physical m_π , continuum limit

[Bali,Bruckmann,Endrödi,Fodor,Katz,Schäfer '12]

Magnetic catalysis – finite temperature

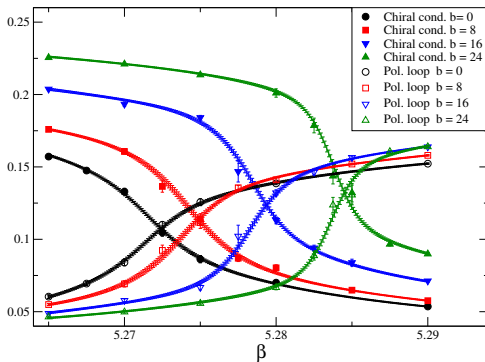
- MC at $T > 0$ seemed a robust concept:
 χ PT, NJL, linear σ , lattice QCD with unphysical m_π



PNJL model [Gatto, Ruggieri '11]

Magnetic catalysis – finite temperature

- MC at $T > 0$ seemed a robust concept:
 χ PT, NJL, linear σ , lattice QCD with unphysical m_π

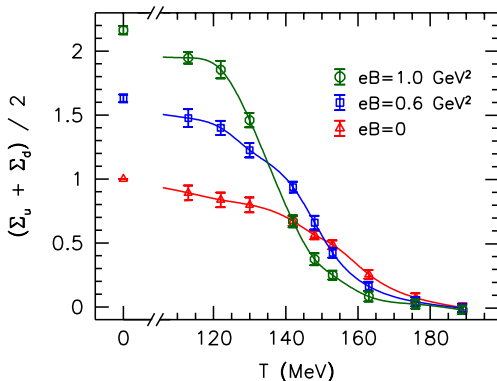


lattice QCD, unphysical m_π , coarse lattice [D'Elia et al '10]

Inverse magnetic catalysis

- lattice QCD, physical m_π , continuum limit

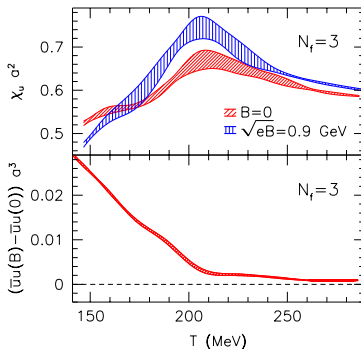
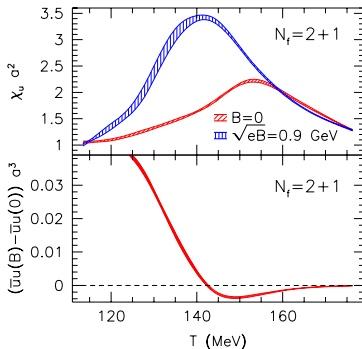
[Bali,Bruckmann,Endrődi,Fodor,Katz,Krieg,Schäfer,Szabó '11, '12]



Inverse magnetic catalysis

- lattice QCD, physical m_π , continuum limit

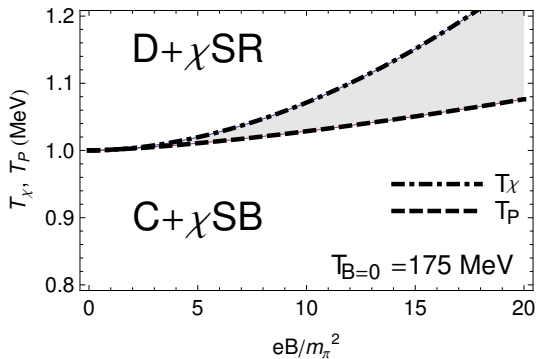
[Bali,Bruckmann,Endrödi,Fodor,Katz,Krieg,Schäfer,Szabó '11, '12]



- IMC disappears if m_π is increased
 $\Rightarrow \exists m_\pi^*$ such that only $m_\pi < m_\pi^*$ gives IMC

Phase diagram

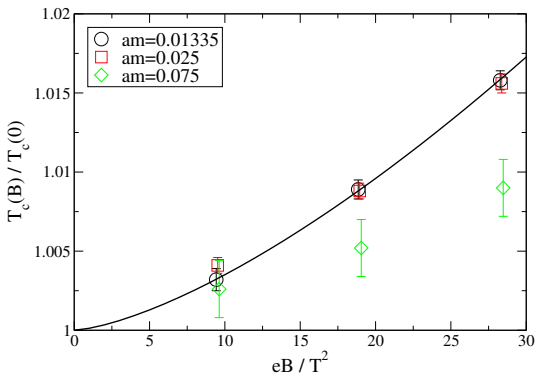
- inflection point of $\bar{\psi}\psi(T)$ defines T_c
- significant difference whether IMC is exhibited or not:



PNJL model [Gatto, Ruggieri '10]

Phase diagram

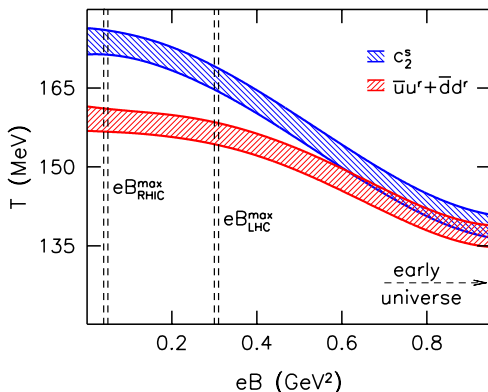
- inflection point of $\bar{\psi}\psi(T)$ defines T_c
- significant difference whether IMC is exhibited or not:



lattice QCD, unphysical m_π , coarse lattice [D'Elia et al '10]

Phase diagram

- inflection point of $\bar{\psi}\psi(T)$ defines T_c
- significant difference whether IMC is exhibited or not:



lattice QCD, physical m_π , continuum limit

[Bali, Bruckmann, Endrődi, Fodor, Katz, Krieg, Schäfer, Szabó '11]

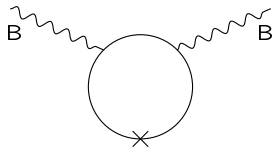
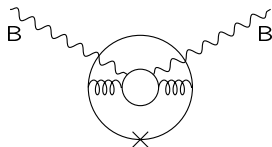
Mechanism behind IMC

- two competing mechanisms at finite B

[Bruckmann, Endrődi, Kovács '13]

- ▶ direct (valence) effect $B \leftrightarrow q_f$
- ▶ indirect (sea) effect $B \leftrightarrow q_f \leftrightarrow g$

$$\bar{\psi}\psi(B) \propto \int \mathcal{D}U e^{-S_g} \underbrace{\det(\not{D}(B, U) + m)}_{\text{sea}} \underbrace{\text{Tr}[(\not{D}(B, U) + m)^{-1}]}_{\text{valence}}$$



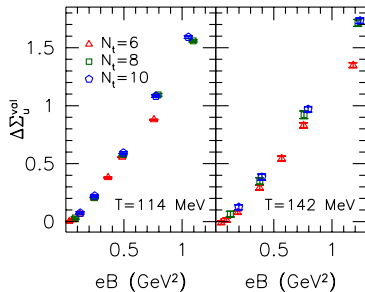
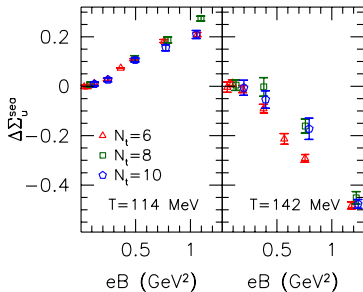
Mechanism behind IMC

- two competing mechanisms at finite B

[Bruckmann, Endrődi, Kovács '13]

- ▶ direct (valence) effect $B \leftrightarrow q_f$
- ▶ indirect (sea) effect $B \leftrightarrow q_f \leftrightarrow g$

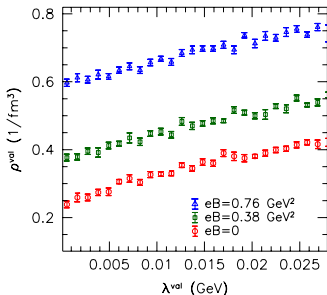
$$\bar{\psi}\psi(B) \propto \int \mathcal{D}U e^{-S_g} \underbrace{\det(\not{D}(B, U) + m)}_{\text{sea}} \underbrace{\text{Tr}[(\not{D}(B, U) + m)^{-1}]}_{\text{valence}}$$



Mechanism behind IMC

- valence sector: driven by the low eigenvalues of \not{D}

$$\bar{\psi}\psi(B) \propto \int \mathcal{D}U e^{-S_g} \prod_i (\lambda_i^2(0) + m^2) \sum_j \frac{m}{\lambda_j^2(B) + m^2}$$



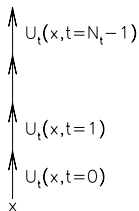
- valence sector: B creates many low eigenvalues through Landau-level degeneracy

Mechanism behind IMC

- sea sector: disfavors low eigenvalues of \mathcal{D} through det

$$\bar{\psi}\psi(B) \propto \int \mathcal{D}U e^{-S_g} \prod_i (\lambda_i^2(B) + m^2) \sum_j \frac{m}{\lambda_j^2(0) + m^2}$$

- most important gauge dof is the Polyakov loop



Mechanism behind IMC

- sea sector: disfavors low eigenvalues of \not{D} through det

$$\bar{\psi}\psi(B) \propto \int \mathcal{D}U e^{-S_g} \prod_i (\lambda_i^2(B) + m^2) \sum_j \frac{m}{\lambda_j^2(0) + m^2}$$

- most important gauge dof is the Polyakov loop



- it represents a shift of the boundary condition \rightarrow influences lowest eigenvalues $\lambda_{\min} \sim P$

Mechanism behind IMC

- sea sector: disfavors low eigenvalues of \not{D} through det

$$\bar{\psi}\psi(B) \propto \int \mathcal{D}U e^{-S_g} \prod_i (\lambda_i^2(B) + m^2) \sum_j \frac{m}{\lambda_j^2(0) + m^2}$$

- most important gauge dof is the Polyakov loop



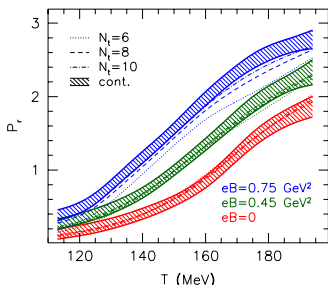
- it represents a shift of the boundary condition \rightarrow influences lowest eigenvalues $\lambda_{\min} \sim P$
- small eigenvalues suppress the determinant (weight)
 $\Rightarrow B$ can increase det through the Polyakov loop

Mechanism behind IMC

- sea sector: disfavors low eigenvalues of \not{D} through det

$$\bar{\psi}\psi(B) \propto \int \mathcal{D}U e^{-S_g} \prod_i (\lambda_i^2(B) + m^2) \sum_j \frac{m}{\lambda_j^2(0) + m^2}$$

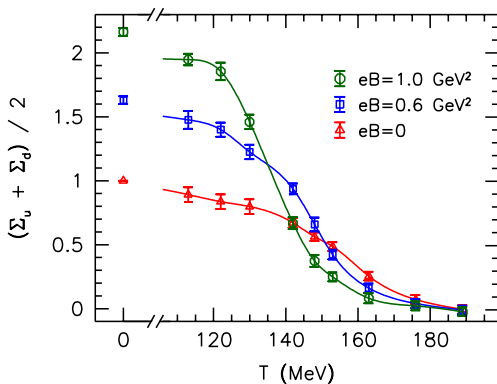
- most important gauge dof is the Polyakov loop



- small eigenvalues suppress the determinant (weight)
 $\Rightarrow B$ can increase det through the Polyakov loop

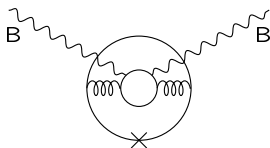
Phase diagram – conclusions

- valence and sea effects compete and around T_c the sea wins



Phase diagram – conclusions

- valence and sea effects compete and around T_c the sea wins
- lessons learned:
 - ▶ LL-picture not applicable to non-perturbative QCD
 - ▶ inclusion of dynamical quarks necessary in the models to reproduce the real phase diagram



- ▶ important to improve effective theories/models (at $\mu_B > 0$ the lattice fails, for example)

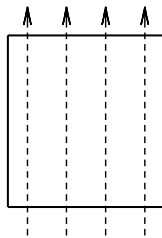
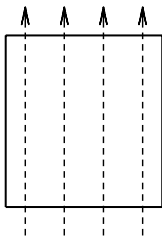
Outline - second part

- numerical results I: phase diagram
 - ▶ symmetries and order parameters
 - ▶ predictions from effective theories and models
 - ▶ magnetic catalysis and inverse catalysis
 - ▶ transition temperature, nature of transition at nonzero B
- numerical results II: equation of state
 - ▶ concept of the pressure in magnetic fields
 - ▶ magnetization, magnetic susceptibility
 - ▶ comparison to hadron resonance gas model
 - ▶ squeezing-effect in heavy-ion collisions
- numerical results III: chiral magnetic effect
 - ▶ electric polarization of CP-odd domains
 - ▶ comparison to model predictions

Concept of pressure at nonzero B

- free energy $\mathcal{F} = -T \log \mathcal{Z}$
- finite volume $V = L_x L_y L_z$, traversed by flux $\Phi = eBL_x L_y$

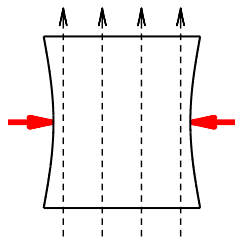
$$p_i = -\frac{1}{V} L_i \frac{d\mathcal{F}}{dL_i}, \quad M = -\frac{1}{V} \frac{1}{e} \frac{\partial \mathcal{F}}{\partial B}$$



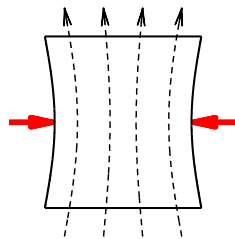
Concept of pressure at nonzero B

- free energy $\mathcal{F} = -T \log \mathcal{Z}$
- finite volume $V = L_x L_y L_z$, traversed by flux $\Phi = e B L_x L_y$

$$p_i = -\frac{1}{V} L_i \frac{d\mathcal{F}}{dL_i}, \quad M = -\frac{1}{V} \frac{1}{e} \frac{\partial \mathcal{F}}{\partial B}$$



$$eB = \text{fix}$$

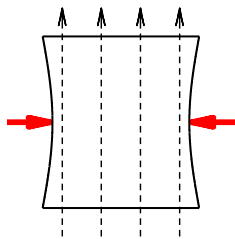


$$\Phi = eB \cdot L_x L_y = \text{fix}$$

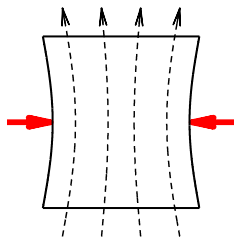
Concept of pressure at nonzero B

- free energy $\mathcal{F} = -T \log \mathcal{Z}$
- finite volume $V = L_x L_y L_z$, traversed by flux $\Phi = eB L_x L_y$

$$p_i = -\frac{1}{V} L_i \frac{d\mathcal{F}}{dL_i}, \quad M = -\frac{1}{V} \frac{1}{e} \frac{\partial \mathcal{F}}{\partial B}$$



$$eB = \text{fix}$$



$$\Phi = eB \cdot L_x L_y = \text{fix}$$

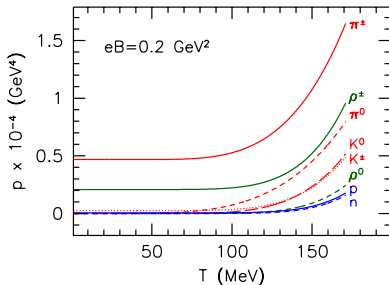
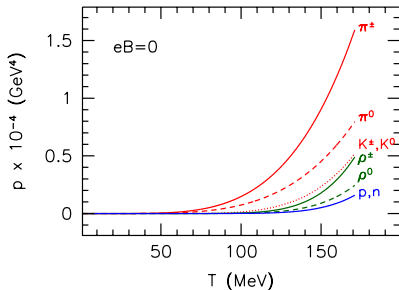
- B -scheme: $p_{x,y}^{(B)} = p_z^{(B)}$, Φ -scheme: $p_{x,y}^{(\Phi)} = p_z^{(\Phi)} - M \cdot eB$

Magnetization from HRG

- hadron resonance gas model: approximate free energy as

$$\mathcal{F} = \sum_h d_h \cdot \mathcal{F}_h^{\text{free}}(m_h, q_h, \sigma_h)$$

QCD input: masses, charges and spins of hadrons

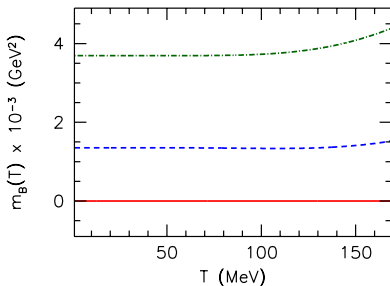
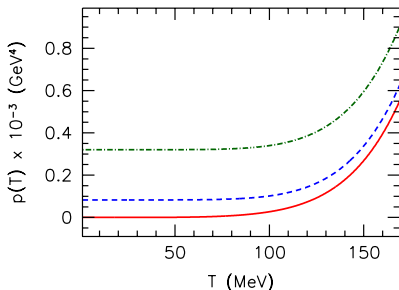


[Endródi '13]

Magnetization from HRG

- equation of state – observables

$$p_z = -\frac{\mathcal{F}}{V}, \quad M = -\frac{1}{V} \frac{\partial \mathcal{F}}{\partial (eB)}, \quad s = -\frac{1}{V} \frac{\partial \mathcal{F}}{\partial T}$$

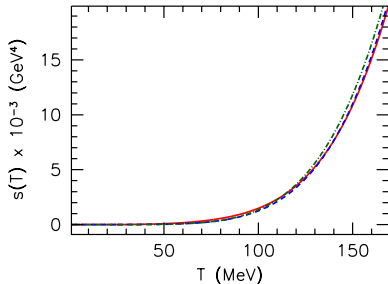
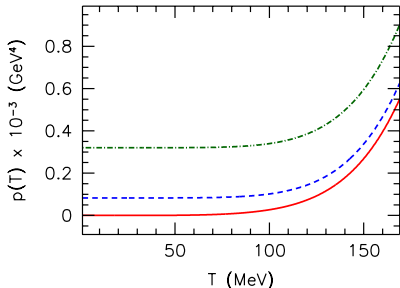


- $M > 0$: QCD vacuum is paramagnetic
- zero- T contribution is a purely quantum effect, it is “created by virtual particles”

Magnetization from HRG

- equation of state – observables

$$p_z = -\frac{\mathcal{F}}{V}, \quad M = -\frac{1}{V} \frac{\partial \mathcal{F}}{\partial (eB)}, \quad s = -\frac{1}{V} \frac{\partial \mathcal{F}}{\partial T}$$



- $M > 0$: QCD vacuum is paramagnetic
- zero- T contribution is a purely quantum effect, it is “created by virtual particles”

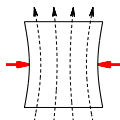
Magnetization from the lattice

- problem with $M \sim \partial\mathcal{F}/\partial B$: magnetic flux is quantized

$$\Phi = qB \cdot L_x L_y = 2\pi \cdot N_b, \quad N_b \in \mathbb{Z}$$

$\Rightarrow B$ -derivative ill defined

\Rightarrow naturally corresponds to the Φ -scheme



- magnetization determined from [Bali, Bruckmann, Endrődi et al '13]

$$p_x - p_z = -M \cdot eB$$

take an anisotropic lattice $\xi = a/a_\alpha$ [Karsch '82]

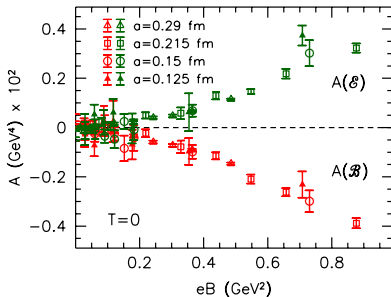
$$p_\alpha = -\xi^2 \frac{T}{V} \frac{d\mathcal{F}}{d\xi} \Big|_a$$

- p_α contains certain components of the QCD action
 $\Rightarrow M \cdot eB$ contains *anisotropies* of the action

Magnetization from the lattice

- anisotropy induced in the gluonic action

$$A(\mathcal{E}) = \frac{1}{2} \left(\text{tr} \mathcal{E}_x^2 + \text{tr} \mathcal{E}_y^2 \right) - \text{tr} \mathcal{E}_z^2, \quad A(\mathcal{B}) = \frac{1}{2} \left(\text{tr} \mathcal{B}_x^2 + \text{tr} \mathcal{B}_y^2 \right) - \text{tr} \mathcal{B}_z^2$$

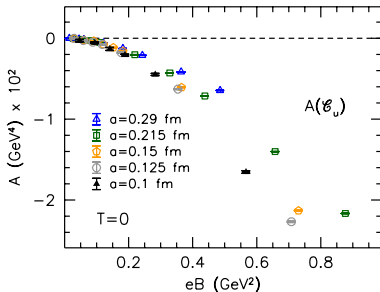


- anisotropy renormalization coefficients also enter here...

Magnetization from the lattice

- dominant contribution is the fermionic anisotropy

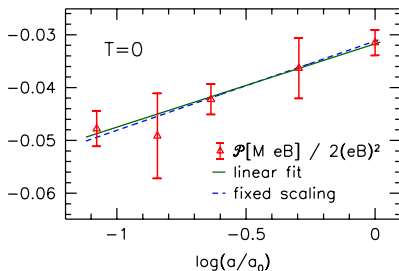
$$M \cdot eB \approx \sum_f A(C_f) = \sum_f \left[\frac{1}{2} \left(\bar{\psi}_f \not{D}_x \psi_f + \bar{\psi}_f \not{D}_y \psi_f \right) - \bar{\psi}_f \not{D}_z \psi_f \right]$$



Magnetization from the lattice

- dominant contribution is the fermionic anisotropy

$$M \cdot eB \approx \sum_f A(C_f) = \sum_f \left[\frac{1}{2} \left(\bar{\psi}_f \not{D}_x \psi_f + \bar{\psi}_f \not{D}_y \psi_f \right) - \bar{\psi}_f \not{D}_z \psi_f \right]$$



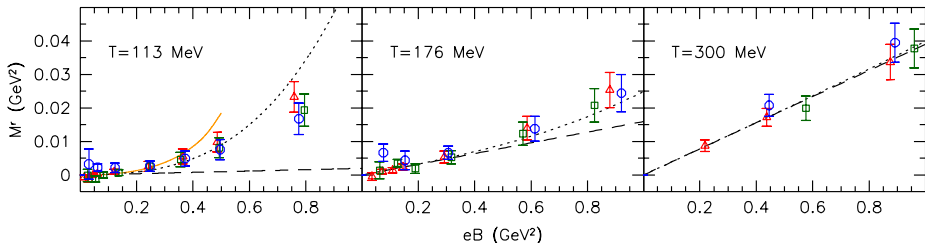
- renormalization

$$M \cdot eB = M^r \cdot eB + 2\beta_1^{\text{QCD}} (eB)^2 \log a,$$

$$\beta_1^{\text{QCD}} = \beta_1 \sum_f \left(\frac{q_f}{e} \right)^2 + \Delta^{\text{QCD}}$$

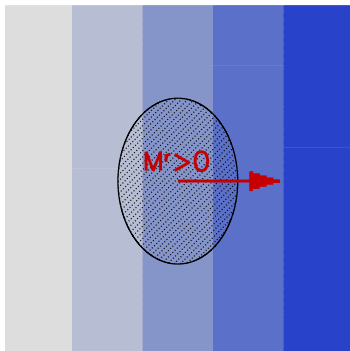
Renormalized magnetization

- subtract $\mathcal{O}((eB)^2)$ term determined at $T = 0$



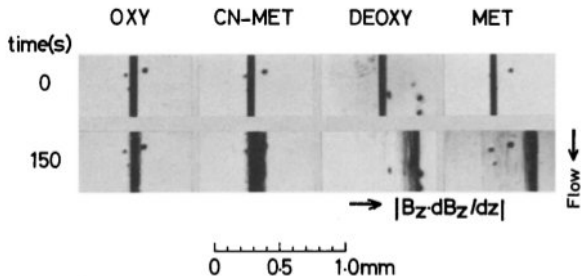
- QCD vacuum is a paramagnet
- compare to hadron resonance gas model at low T
- linear response $M^r = \chi_1 \cdot eB$ gets stronger above T_c

Paramagnetism and inhomogeneous fields



- $-\partial\mathcal{F}^r/\partial(eB) = M^r > 0$
 \Rightarrow free energy \mathcal{F}^r minimized in the region where B is maximal

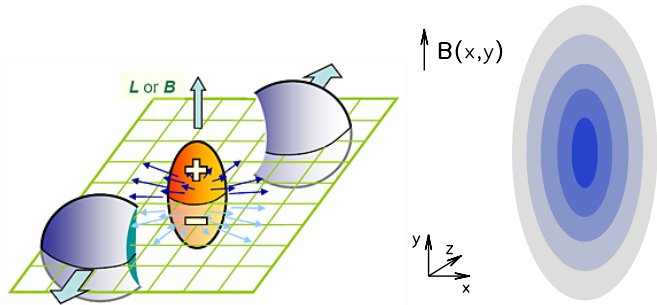
Paramagnetism - blood cells



- red blood cells displaced more if they contain more (paramagnetic) haemoglobin [Okazaki et al '87]

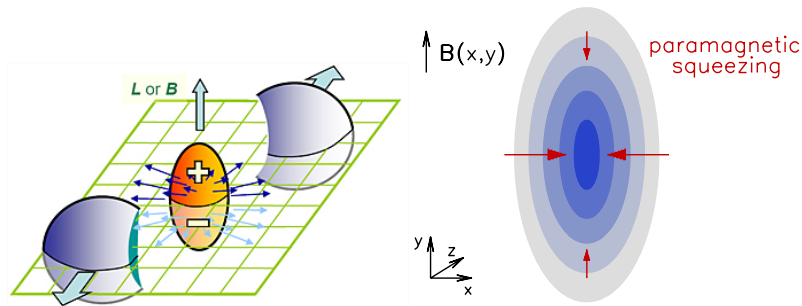
Paramagnetism - heavy ions

- take a non-central heavy-ion collision
 \hat{z} : beam direction, \hat{x} - \hat{y} : transverse plane, \hat{x} : impact parameter



Paramagnetism - heavy ions

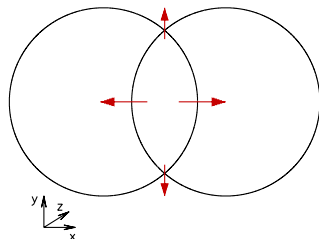
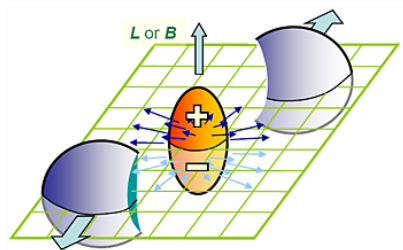
- take a non-central heavy-ion collision
 \hat{z} : beam direction, \hat{x} - \hat{y} : transverse plane, \hat{x} : impact parameter



- free energy minimization squeezes QCD matter anisotropically
 [Bali,Bruckmann,Endrödi,Schäfer '13]

Paramagnetism - heavy ions

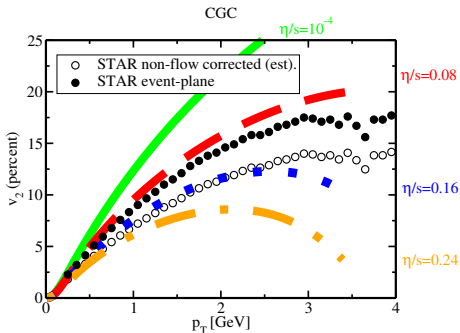
- take a non-central heavy-ion collision
 \hat{z} : beam direction, \hat{x} - \hat{y} : transverse plane, \hat{x} : impact parameter



- elliptic flow: anisotropic pressure gradients due to initial geometry

Elliptic flow

- robust effect in non-central collisions
- integrated v_2 used to extract η/s



[Luzum, Romatschke '08]

Elliptic flow vs paramagnetic squeezing

- the force density produced through paramagnetism:

$$F^{\text{PS}} = -\nabla \mathcal{F}^r = -\frac{\partial \mathcal{F}^r}{\partial (eB)} \cdot \nabla (eB) = M^r \cdot \nabla (eB).$$

- simplistic way to quantify it:

$$\Delta p'_{\text{ps}} = F^{\text{PS}}(\sigma_x, 0) - F^{\text{PS}}(0, \sigma_y)$$

- ▶ RHIC: $|\Delta p'_{\text{ps}}| \approx 0.007 \text{ GeV/fm}^4$
 - ▶ LHC: $|\Delta p'_{\text{ps}}| \approx 0.7 \text{ GeV/fm}^4$
- effect due to initial geometry
[Kolb et al '00; Petersen et al '06; Huovinen]
 - ▶ RHIC: $|\Delta p'_g| \approx 0.1 \text{ GeV/fm}^4$
 - ▶ LHC: $|\Delta p'_g| \approx 1 \text{ GeV/fm}^4$

Elliptic flow vs paramagnetic squeezing

- the force density produced through paramagnetism:

$$F^{\text{PS}} = -\nabla \mathcal{F}^r = -\frac{\partial \mathcal{F}^r}{\partial (eB)} \cdot \nabla (eB) = M^r \cdot \nabla (eB).$$

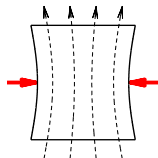
- simplistic way to quantify it:

$$\Delta p'_{\text{ps}} = F^{\text{PS}}(\sigma_x, 0) - F^{\text{PS}}(0, \sigma_y)$$

- ▶ RHIC: $|\Delta p'_{\text{ps}}| \approx 0.007 \text{ GeV/fm}^4 \leftarrow \sim 7\% \text{ correction?}$
 - ▶ LHC: $|\Delta p'_{\text{ps}}| \approx 0.7 \text{ GeV/fm}^4 \leftarrow \sim 70\% \text{ correction?}$
- effect due to initial geometry
[Kolb et al '00; Petersen et al '06; Huovinen]
 - ▶ RHIC: $|\Delta p'_g| \approx 0.1 \text{ GeV/fm}^4$
 - ▶ LHC: $|\Delta p'_g| \approx 1 \text{ GeV/fm}^4$

Equation of state – conclusions

- at $B > 0$, pressure depends on the scheme (B vs Φ)
- QCD vacuum is paramagnetic (free quarks in SB limit; HRG; lattice QCD with physical m_π)
- at $T = 0$ this is a pure quantum effect; it produces no entropy
- paramagnetism + non-uniform fields = squeezing effect
 - ▶ in heavy-ion collisions: competes with elliptic flow
 - ▶ crude estimate: it might be important
 - ▶ future model descriptions: take into account $B(x, y, t)$ and compare the two effects more carefully

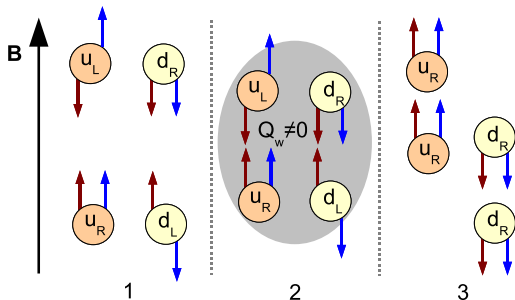


Outline - second part

- numerical results I: phase diagram
 - ▶ symmetries and order parameters
 - ▶ predictions from effective theories and models
 - ▶ magnetic catalysis and inverse catalysis
 - ▶ transition temperature, nature of transition at nonzero B
- numerical results II: equation of state
 - ▶ concept of the pressure in magnetic fields
 - ▶ magnetization, magnetic susceptibility
 - ▶ comparison to hadron resonance gas model
 - ▶ squeezing-effect in heavy-ion collisions
- numerical results III: chiral magnetic effect
 - ▶ electric polarization of CP-odd domains
 - ▶ comparison to model predictions

Chiral magnetic effect

- local CP-violation through domains with $Q_{\text{top}} \neq 0$?
- detect them through magnetic field B [Kharzeev et al. '08]

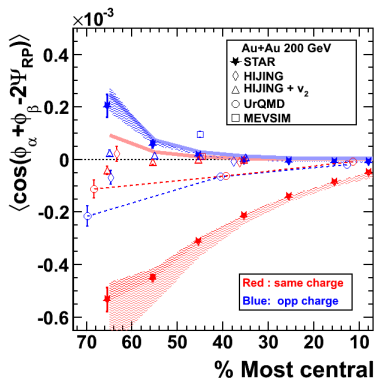
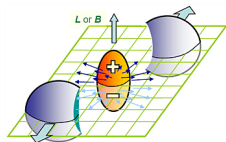


1. quarks interact with B : spins aligned
2. quarks interact with topology: chiralities (helicities) “aligned”
3. result: charge separation

Chiral magnetic effect

- Q_{top} -domains fluctuate, direction of B fluctuates
 \Rightarrow effect vanishes on average
- correlations may survive ($\alpha, \beta = \pm$)

$$a_{\alpha\beta} = -\cos[(\Phi_\alpha - \Psi_{\text{RP}}) + (\Phi_\beta - \Psi_{\text{RP}})]$$



[STAR collaboration '09]

- need 3-particle correlations (technically complicated)
- CME prediction:

$$a_{++} = a_{--} = -a_{+-} > 0$$
- CP-even backgrounds should be subtracted

Polarization of θ -domains

- magnetic/electric field induces magnetic/electric polarization

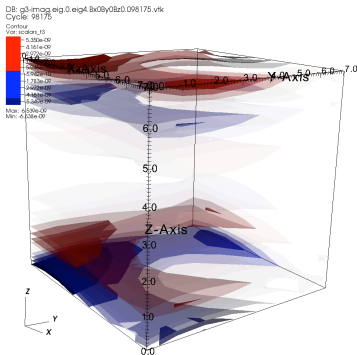
$$\bar{\psi}_f \sigma_{\mu\nu} \psi_f \propto q_f F_{\mu\nu}, \quad \sigma_{\mu\nu} = [\gamma_\mu, \gamma_\nu]/2i$$

- in the presence of topology, the roles are exchanged

$$\epsilon_{\mu\nu\alpha\beta} Q_{\text{top}} \cdot \bar{\psi}_f \sigma_{\alpha\beta} \psi_f \propto q_f F_{\mu\nu}$$

- put instanton configuration ($Q_{\text{top}} = 1$) on the lattice and expose it to magnetic field ($B = F_{xy}$)

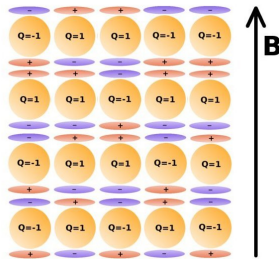
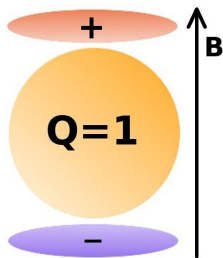
[Abramczyk et al '09]



Polarization of θ -domains

- QCD vacuum: no instanton but local fluctuations in q_{top}
- polarization exhibits a local correlation
[Bali,Bruckmann,Endrödi,Fodor,Katz,Schäfer '14]

$$\left\langle \int d^4x q_{\text{top}}(x) \cdot \bar{\psi}_f \sigma_{zt} \psi_f(x) \right\rangle \propto q_f F_{xy}$$



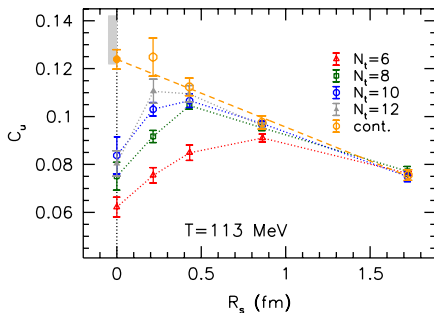
Polarization of θ -domains

- lattice approach
 - ▶ measure the correlator at physical m_π
 - ▶ renormalization involves smearing of fields over a range R_s
 - ▶ extrapolate to continuum limit and to $R_s \rightarrow 0$
- model description
 - ▶ assume q_{top} is generated by constant self-dual background fields $G_{xy} = G_{zt}$ (parallel to magnetic field F_{xy})
 - ▶ neglect quark masses $m^2 \ll F, G \leftrightarrow$ LLL approximation
 - ▶ assume normal distribution for q_{top}
- consider the dimensionless combination

$$C_f = \frac{\langle q_{\text{top}}(x) \cdot \bar{\psi}_f \sigma_{zt} \psi_f(x) \rangle}{\sqrt{\langle q_{\text{top}}^2(x) \rangle \langle \bar{\psi}_f \sigma_{xy} \psi_f(x) \rangle}}$$

Polarization of θ -domains

- model: $C_f \sim 1 \Rightarrow B$ -polarization equals E -polarization for unit topology
- lattice: $C_f \sim 0.13$

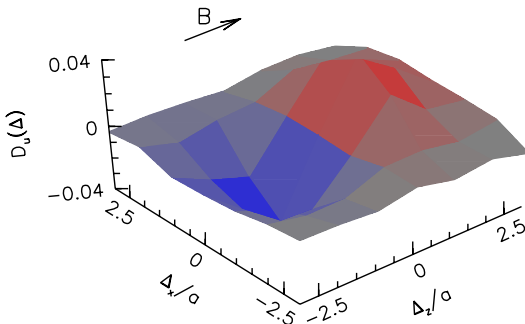


\Rightarrow non-perturbative QCD interactions prevent full electric polarization of the quarks (for massive quarks spin flip becomes possible)

Electric charge separation

- the localized electric dipole moment is related to an extended charge structure

$$D_f(\Delta) = \left\langle \int d^4x q_{\text{top}}(x) \cdot \bar{\psi}_f \gamma_0 \psi_f(x + \Delta) \right\rangle \propto q_f B, \quad \text{if } \Delta \parallel B$$



CME - conclusions

- local CP violation induced through $B +$ fluctuating $q_{\text{top}}(x)$
- usual assumptions (LLL, massless quarks) overestimate strength of local CP violation by order of magnitude

Summary

